NASA/TM—2006-213968

Observations of a Cast Cu-Cr-Zr Alloy

David L. Ellis
Glenn Research Center, Cleveland, Ohio

February 2006

NASA STI Program . . . in Profile

Since its founding, NASA has been dedicated to the advancement of aeronautics and space science. The NASA Scientific and Technical Information (STI) program plays a key part in helping NASA maintain this important role.

The NASA STI Program operates under the auspices of the Agency Chief Information Officer. It collects, organizes, provides for archiving, and disseminates NASA's STI. The NASA STI program provides access to the NASA Aeronautics and Space Database and its public interface, the NASA Technical Reports Server, thus providing one of the largest collections of aeronautical and space science STI in the world. Results are published in both non-NASA channels and by NASA in the NASA STI Report Series, which includes the following report types:

- TECHNICAL PUBLICATION. Reports of completed research or a major significant phase of research that present the results of NASA programs and include extensive data or theoretical analysis. Includes compilations of significant scientific and technical data and information deemed to be of continuing reference value. NASA counterpart of peer-reviewed formal professional papers but has less stringent limitations on manuscript length and extent of graphic presentations.

- TECHNICAL MEMORANDUM. Scientific and technical findings that are preliminary or of specialized interest, e.g., quick release reports, working papers, and bibliographies that contain minimal annotation. Does not contain extensive analysis.

- CONTRACTOR REPORT. Scientific and technical findings by NASA-sponsored contractors and grantees.

- CONFERENCE PUBLICATION. Collected papers from scientific and technical conferences, symposia, seminars, or other meetings sponsored or cosponsored by NASA.

- SPECIAL PUBLICATION. Scientific, technical, or historical information from NASA programs, projects, and missions, often concerned with subjects having substantial public interest.

- TECHNICAL TRANSLATION. English-language translations of foreign scientific and technical material pertinent to NASA's mission.

Specialized services also include creating custom thesauri, building customized databases, organizing and publishing research results.

For more information about the NASA STI program, see the following:

- Access the NASA STI program home page at *http://www.sti.nasa.gov*

- E-mail your question via the Internet to *help@sti.nasa.gov*

- Fax your question to the NASA STI Help Desk at 301–621–0134

- Telephone the NASA STI Help Desk at 301–621–0390

- Write to:
  NASA STI Help Desk
  NASA Center for AeroSpace Information
  7121 Standard Drive
  Hanover, MD 21076–1320

NASA/TM—2006-213968

Observations of a Cast Cu-Cr-Zr Alloy

David L. Ellis
Glenn Research Center, Cleveland, Ohio

National Aeronautics and
Space Administration

Glenn Research Center
Cleveland, Ohio 44135

February 2006

Level of Review: This material has been technically reviewed by technical management.

Available from

NASA Center for Aerospace Information
7121 Standard Drive
Hanover, MD 21076–1320

National Technical Information Service
5285 Port Royal Road
Springfield, VA 22161

Available electronically at http://gltrs.grc.nasa.gov

Observations of a Cast Cu-Cr-Zr Alloy

David L. Ellis
National Aeronautics and Space Administration
Glenn Research Center
Cleveland, Ohio 44135

Abstract

Prior work has demonstrated that Cu-Cr-Nb alloys have considerable advantages over the copper alloys currently used in regeneratively cooled rocket engine liners. Observations indicated that Zr and Nb have similar chemical properties and form very similar compounds. Glazov and Zakharov et al. reported the presence of Cr_2Zr in Cu-Cr-Zr alloys with up to 3.5 wt% Cr and Zr though Zeng et al. calculated that Cr_2Zr could not exist in a ternary Cu-Cr-Zr alloy. A cast Cu-6.15 wt% Cr-5.25 wt% Zr alloy was examined to determine if the microstructure developed would be similar to GRCop-84 (Cu-6.65 wt% Cr-5.85 wt% Nb). It was observed that the Cu-Cr-Zr system did not form any Cr_2Zr even after a thermal exposure at 875 °C for 176.5 h. Instead the alloy consisted of three phases: Cu, Cu_5Zr, and Cr.

Introduction

High-conductivity materials with good high-temperature strength, creep resistance, and low-cycle fatigue (LCF) lives are needed for a variety of regeneratively cooled rocket engine applications especially main combustion chamber liners. Work at the NASA Glenn Research Center (refs. 1 to 3) has focused on Cu-Cr-Nb alloys such as GRCop-84, which offer great promise for these and other high-temperature heat exchanger applications.

The Cu-Cr-Nb system was selected because Cr and Nb have minimal solubility in solid copper (refs. 4 and 5) but high solubility in liquid copper. They also form a high-melting-point intermetallic compound, Cr_2Nb (ref. 6). Utilizing rapid solidification technology, a very fine dispersion of Cr_2Nb, can be formed in a nearly pure copper matrix. This dispersion gives Cu-Cr-Nb alloys such as GRCop-84 (Cu-6.65 wt% Cr-5.85 wt% Nb) an excellent combination of strength, creep resistance, fatigue life, conductivity, and thermal expansion (ref. 7).

Comparing the mechanical properties of pure copper to AMZIRC, a commercial Cu-0.15 wt% Zr alloy, revealed that the small addition of Zr greatly improved the properties of the alloy above pure copper. Of particular interest was the increase in softening temperature (refs. 8 and 9) and LCF lives (refs. 9 and 10) relative to pure copper that the small addition of Zr to Cu causes.

The Cr-Zr phase diagram (ref. 11) shows that Cr and Zr develop the intermetallic compound Cr_2Zr. It is assumed that, like Cr_2Nb, the intermetallic compound will be hard and suitable for strengthening Cu. Both Cr_2Zr and Cr_2Nb have C_{15} cubic structures (refs. 12 and 13) and an Fd3m or Cu_2Mg space group. The lattice parameters of Cr_2Zr and Cr_2Nb are 0.721 and 0.7659 nm, respectively. These similarities in structures and unit cell sizes between the two compounds held promise for producing a microstructure with Cu and Cr_2Zr.

While the Cu-Zr phase diagram (ref. 14) shows that more Zr can dissolve into solid copper than Nb, the amount is still small at approximately 0.1 at.%. The potential removal of any trace oxygen from the copper matrix by the Zr could compensate for any decrease in conductivity from dissolved Zr as well.

Limited prior work on the Cr-Cu-Zr phase diagram had been conducted in the 1950s. Glazov et al. (refs. 15 and 16) and Zakharov et al. (ref. 17) determined that, in alloys with up to 3.5 wt% Cr and 3.5 wt% Zr, Cr_2Zr could form. They postulated a Cu-Cr_2Zr pseudobinary phase diagram. More recent work, in particular the papers by Zeng et al. (refs. 18 and 19), have shown that Cr_2Zr will not form in the Cr-Cu-Zr ternary system. An isothermal section of the Cr-Cu-Zr ternary phase diagram calculated by

Zeng is shown in figure 1. Instead three phases—Cu, Cr, and Cu_5Zr—will be present up to 25 at.% Cr along the Cu-Cr_2Zr vertical section of the ternary phase diagram.

The success of the Cu-Cr-Nb alloys developed at NASA Glenn led to the desire to revisit the Cu-Cr-Zr alloys. A Cu-Cr-Zr alloy modeled after GRCop-84 with Zr directly substituting for Nb could have at least two potential advantages over the comparable Cu-Cr-Nb alloy. The Cr_2Zr should dissolve into the liquid copper at a lower temperature than Cr_2Nb. This could decrease the melt temperatures and make powder production significantly easier. If an excess of Zr is added, then the Zr in the copper matrix could act to retard the softening of the alloy at high temperatures following cold work as it does in AMZIRC. The addition of Zr should also improve LCF lives, a major necessity for rocket engine liners.

To determine if Cu-Cr-Zr alloys could form an alloy consisting of a Cu-rich matrix strengthened by Cr_2Zr precipitates, a Cu-Cr-Zr alloy was cast and analyzed for the phases present in the as-cast condition and following a high-temperature heat treatment designed to achieve equilibrium among the phases.

Experimental Procedure

The theoretical density of Cr_2Zr was calculated based upon the crystallographic data available for the low-temperature form of the phase (ref. 13). Using this calculated density and the density of copper, a composition of Cu-6.0 wt% Cr-5.4 wt% Zr was calculated to give 14 vol% Cr_2Zr. On an atomic basis, this composition corresponds to Cu-7.4 at.% Cr-3.7 at.% Zr and gives the desired 2:1 atomic ratio of Cr to Zr needed for stochiometric Cr_2Zr. No correction to this composition was made to compensate for anticipated losses in Cr and Zr during the casting process or any solubility of Cr and Zr in the copper matrix. As shown in figure 1, this composition lies along the Cu-Cr_2Zr line.

A charge of elemental Cu, Cr, and Zr with this composition was melted using induction melting under an argon cover gas. All materials used had at least 99.9 percent purity. The molten metal was poured into a solid copper mold with a nominal cavity dimension of 25.4 by 50.8 by 76.2 mm (1 by 2 by 3 in.). Following casting samples were submitted for chemical analysis.

The casting was cut into blocks approximately 1.9 by 1.3 by 1.3 cm (0.75 by 0.5 by 0.5 in.) and examined metallographically. The samples were polished and examined in the scanning electron microscope (SEM). Backscattered electron (BSE) imaging was used to qualitatively determine the location of the elements and phases present in the casting. It was also possible to use the images to quantitatively determine the volume fraction of each phase. Energy dispersion spectroscopy (EDS) was used to semiquantitatively determine the composition of each phase observed.

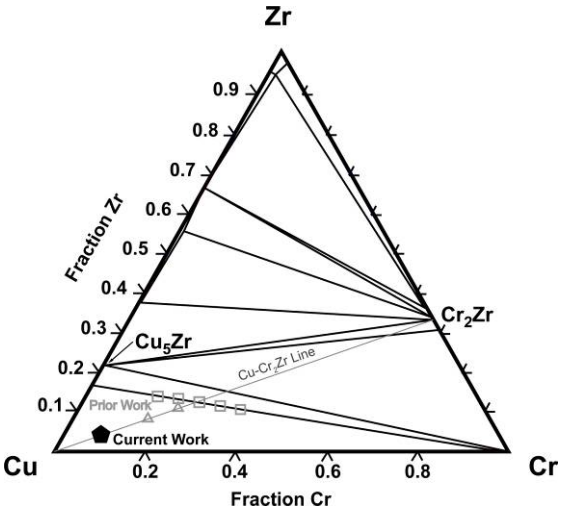

Alloy	Cu	Cr	Zr
CUZR–1	70.0	16.0	14.0
CUZR–2	65.8	21.0	13.2
CUZR–3	61.7	26.0	12.3
CU ZR–4	57.5	31.0	11.5
CUZR–5	53.3	36.0	10.7
CRZR–1	75.0	16.7	8.3
CRZR–2	67.0	22.0	11.0
Current study	**88.9**	**7.4**	**3.7**

Figure 1.—Calculated Cr-Cu-Zr phase diagram at 940 °C adapted from Zeng et al. (ref. 18) and alloy compositions.

To determine the volume fraction of each phase present, BSE images of the alloy were analyzed using SigmaScan image analysis software. The picture was divided into three parts based upon the grayscale intensity of each pixel. This delineated the three phases well except in the fine lamella and at the boundaries of some particles. This introduces a small error judged to be much less than 5 percent of the measured values. The total pixels for each phase were counted and divided by the total pixels counted to give an area fraction for each phase. Five images were used to calculate the area fraction of each phase. The area fraction is equal to the volume fraction of each phase.

Microprobe analysis was conducted on the as-cast sample to achieve a quantitative analysis of each phase. A JEOL 8200 Superprobe with five wavelength dispersive spectrometers (WDSs) and one EDS detector allowed for simultaneous measurement of all three major elements of interest. In addition to the quantitative analysis of each phase, additional BSE images and x-ray maps were obtained. X-ray diffraction was performed on a sample using a Phillips APD3600 Automatic Powder Diffractometer to determine the crystallography of the phases present as well.

After examination of the as-cast material, a sample was cut from the casting and exposed at 875 °C (1607 °F) for 176.5 h and air cooled (AC) to determine if Cr_2Zr would form during a heat treatment through diffusion and reaction between the Cr and Zr. Samples were examined using the SEM and x-ray diffraction to determine phase and microstructural changes.

Results

The casting had detectable internal porosity, but little shrinkage or piping was noted in the central core. It is believed that the porosity is gas porosity caused by dissolved hydrogen introduced through the zirconium metal that did not have time to escape from the melt before casting into the mold.

The overall composition of the alloy is shown in table 1. In addition to the three main constituents, some trace contaminants were also detected. Their levels are low and should not affect any of the results. No additional elements beyond those listed were detectable using inductively coupled plasma spectroscopy.

Calculated volume fraction is computed from the Cr-Cu-Zr phase diagram (ref. 18) using lever rule. X-ray diffraction determined that three phases were present—elemental Cr, elemental Cu, and Cu_5Zr. No Cr_2Zr was detected.

SEM examination with both secondary electrons (SEs) and (BSEs) revealed a microstructure with three distinct and easily observed regions. Examples of both types of images are shown in figures 2 and 3. For comparison purposes, an optical micrograph of a similarly cast Cu-Cr-Nb alloy microstructure is presented in figure 3. Large Cr_2Nb precipitates are easily visible, and there is no evidence of elemental Cr in the Cu-Cr-Nb alloy.

TABLE 1.—COMPOSITION OF Cu-Cr-Zr CASTING

Element	Weight percentage
Cu	Bal.
Cr	6.15
Zr	5.25
Fe	30 ppm
N	6 ppm
O	159 ppm
S	10 ppm
Y	150 ppm

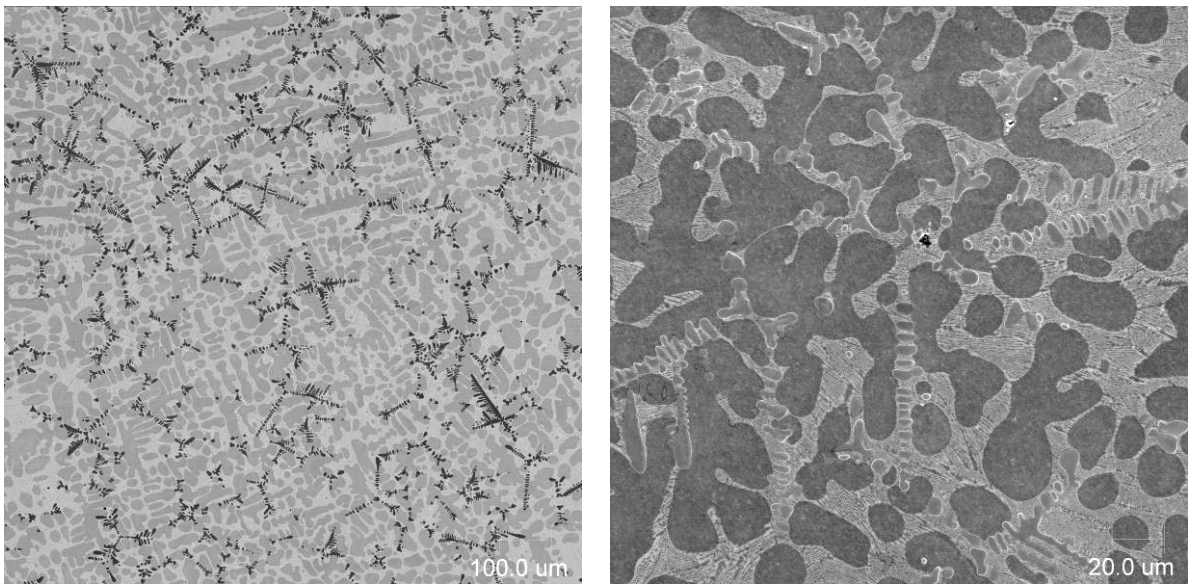

(a) (b)

Figure 2.—Overall microstructure of as-cast Cu-6.0 Cr-5.4 Zr alloy (a) BSE image (b) SE image.

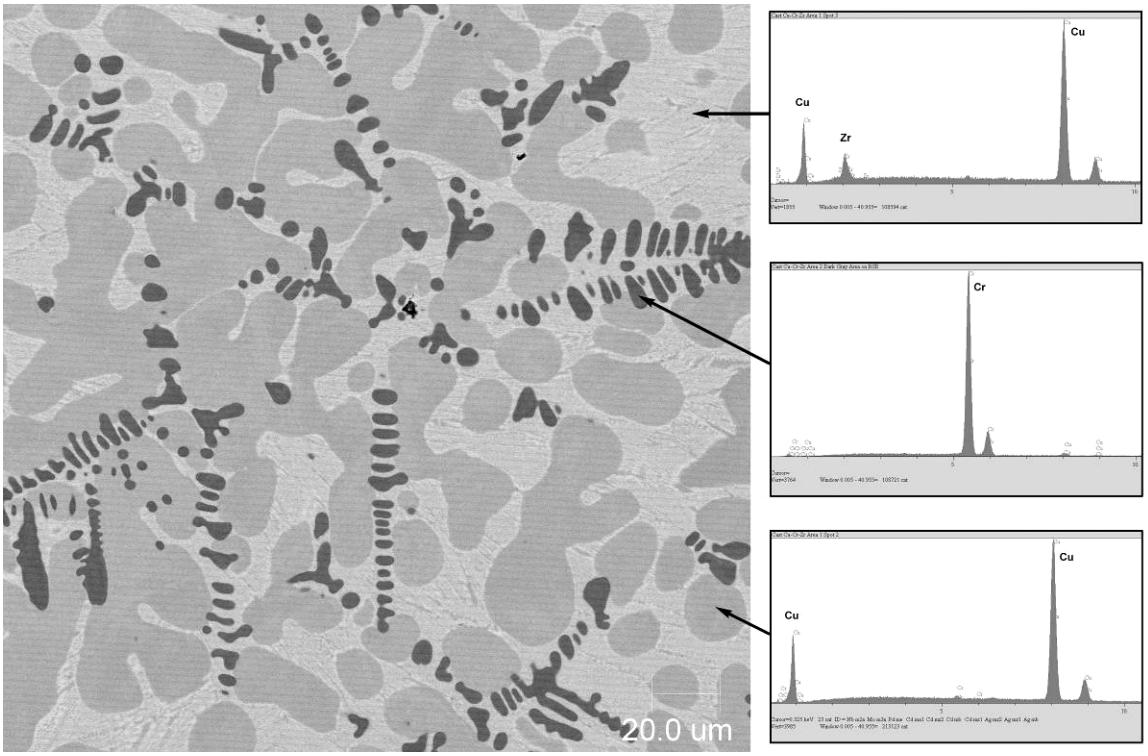

Figure 3.—Detail of general microstructure (BSE image) with EDS spectra. Same area as in figure 2.

Using EDS and the information from the x-ray diffraction results, the observed regions were identified as elemental Cr dendrites, elemental Cu dendrites, and Cu-Cu_5Zr in the interdendritic spaces. The measured volume fractions for each phase are listed in table 2. The Cu-Zr phase revealed a very fine lamellar structure as seen in figure 4. The Cr and Cu have a larger, dendritic structure. Based upon this structure and the various melting points, it is surmised that the Cr solidified first followed by the Cu. The remaining Zr-rich liquid solidified last.

TABLE 2.—VOLUME FRACTION OF EACH PHASE

Phase	Measured volume fraction	Calculated volume fraction
Cr	10.1%	8.1%
Cu	62.0%	67.6%
Cu_5Zr	27.9%	24.3%

Calculated volume fraction is computed from the Cr-Cu-Zr phase diagram (ref. 18) using lever rule.

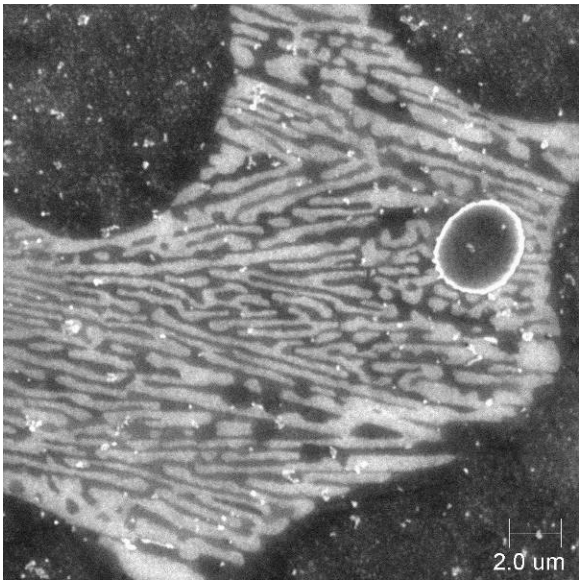

Figure 4.—Fine Cu-Cu_5Zr lamellar structure.

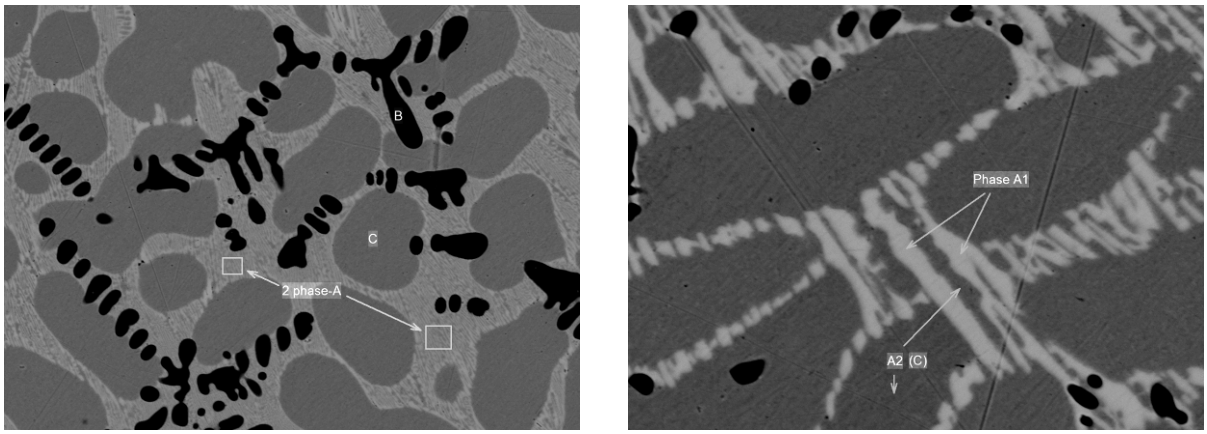

Figure 5.—BSE images showing features analyzed by microprobe.

Quantitative microprobe analysis was performed on each phase. Representative images of the areas analyzed are shown in figure 5. The quantitative results are shown in table 3. For the lamellae, the microprobe's resolution enabled the analysis of the two different phases individually in regions where the lamellae were somewhat coarser than average or had an above-average spacing. These results were judged to be representative of the finer lamellae as well.

TABLE 3.—MICROPROBE QUANTITATIVE CHEMICAL ANALYSIS RESULTS

Microstructural feature	Cu (wt%/at.%)	Cr (wt%/at.%)	Zr (wt%/at.%)	Phase(s)
Overall lamellae (phase A)	88.4/90.6	0.5/0.6	12.0/8.6	Cu + Cu_5Zr
Light lamella (phase A1)	76.9/82.1	0.7/1.0	22.7/16.9	Cu_5Zr
Dark lamella (phase A2)	99.1/99.0	0.6/0.8	0.3/0.2	Cu
Cr dendrites (phase B)	2.4/2.0	97.4/98.0	0.0/0.0	Cr
Cu dendrites (phase C)	99.3/99.4	0.1/0.1	0.4/0.6	Cu

All results are the average of analysis of five different features.

The microstructure of the Cu-Cr-Zr alloy after a 176.5-h heat treatment at 875 °C is shown in figures 6 and 7. The elemental Cr dendrites appear to be unaffected by the high-temperature exposure. The solid solubility of Cr in pure Cu is only 0.1 wt% at 875 °C, so it was not expected that the Cr dendrites would dissolve. However, it was hoped that the rapid diffusion of Cr in Cu would lead to transport of Cr to Zr and the reaction of the two elements to form Cr_2Zr. No Cr_2Zr was detected in the specimen even in regions where Cr- and Zr-rich phases were in intimate contact. The Cu-Cu_5Zr lamellar structure has been replaced with what appears to be a uniform phase even at ×10 000. In all probability the areas contain very fine Cu_5Zr uniformly dispersed within a copper matrix.

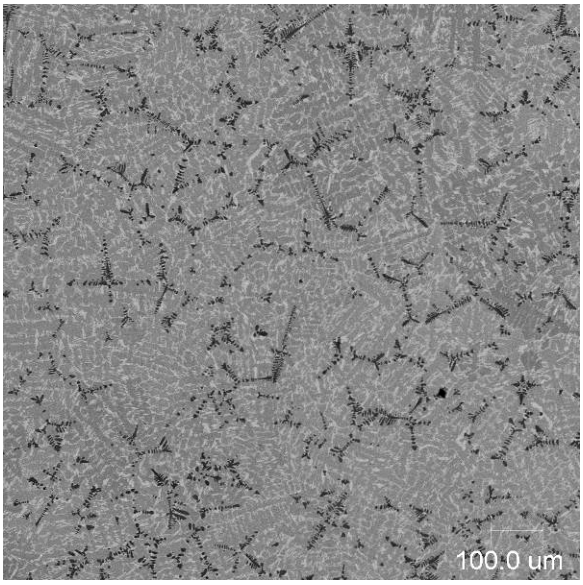

Figure 6.—Overall microstructure of Cu-6.0 Cr-5.4 Zr alloy following 875 °C (1607 °F)/ 176.5 h/AC thermal exposure (BSE).

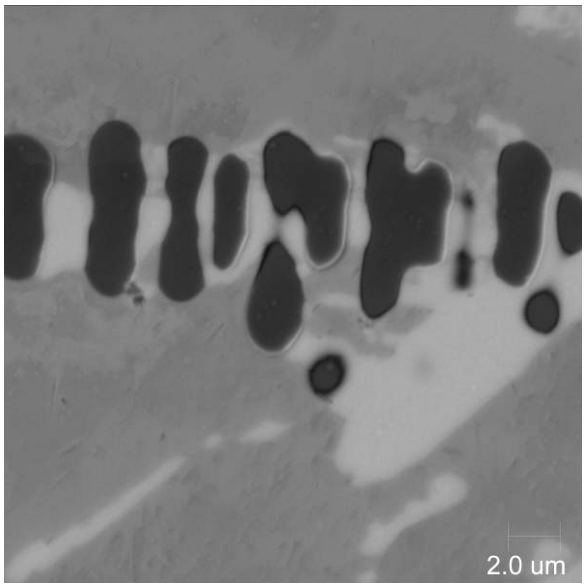

Figure 7.—Detail of area with Cr and Cu_5Zr in intimate contact following thermal exposure illustrating lack of observable reaction and disappearance of lamellae (BSE).

Discussion

Unfortunately, both the EDS and x-ray diffraction results confirm that there was no detectable amount of Cr_2Zr formed in the casting process. While Zr, element 40, and Nb, element 41, share many similarities, the small differences such as electronegativity (1.33 versus 1.6 on Pauling scale (ref. 20)) appear to be sufficiently great to prevent the ready formation of Cr_2Zr in the presence of copper during a conventional casting process.

Exposure of the cast alloy to 875 °C or 0.96 T_m based upon the Cu-Cr_9Zr_2 eutectic temperature of 927 °C (ref. 14) did not promote the formation for Cr_2Zr. The only detectable microstructural change observed was the Cu and Cu_5Zr lamellae disappearing and the formation of a uniform Cu_5Zr phase with no resolvable details at ×10 000 magnification. This applied even when the Cr and Cu_5Zr phases were in intimate contact.

The presence of the Cu_5Zr phase is at odds with the refereed Cu-Zr phase diagram of Arias and Abriata (ref. 14), which is based on thermodynamic and experimental data. They show the phase that should be present is Cu_9Zr_2. Cu_4Zr (ref. 21), Cu_9Zr_2 (refs. 22 and 23), and Cu_5Zr (refs. 24 to 26) have been reported by various researchers and which composition is correct continues to be a point of some contention. In this study the composition of the phase on an atomic basis had an average Cu to Zr ratio of 4.86. The presence of a Cu matrix should tend to bias the Cu to Zr ratio from the microprobe results lower due to the excitation volume of the probe beam including the adjacent Cu-rich phase. The x-ray diffraction analysis peaks correspond accurately with the published values for Cu_5Zr (ref. 27) indicating it had the proper lattice structure and lattice parameters for this phase as well.

It needs to be noted that the presence of the third element, Cr, will affect the activity of both the Cu and Zr. It is known that both Cr and Zr have limited solid solubility in Cu. At 875 °C, the solid solubility is approximately 0.1 at.% for both Cr and Zr (refs. 11, 14, 18, and 19). That would result in a lowering of the activity of Cu to 0.998 if Raoultian behavior is assumed for simplicity. Interactions between the Cr and Zr may introduce nonideal behavior, which would require determination of the activity coefficients for the three elements, but the small magnitude of both concentrations in copper would probably not result in any significant change from the Raoultian value.

Zeng et al. (ref. 18) calculated the complete Cr-Cu-Zr phase diagram including the Zr-rich corner. Their results indicate that several atomic percent of Cr and Zr can dissolve into Zr. At 875 °C, the approximate amount of Cr and Cu that can be dissolved into Zr are 3.5 and 4 at.%, respectively. Assuming Raoultian behavior, the activity of the Zr would be reduced to 0.925. The solid solution is also sufficiently concentrated that nonideal behavior is likely, which could change the Zr activity further. This change in activity and corresponding shifts in the free energies of formation may account for the observed presence of Cu_5Zr instead of Cu_9Zr_2.

The compositional and phase results of this study are consistent with those obtained by Zeng et al. (ref. 19). Their reported values for the composition of the Cr and Cu_5Zr phases for four of their alloys obtained using a Noran Voyager II EDS system with a PROZA-correction system are almost identical to the microprobe compositions obtained in this study.

The volume fraction of each phase was calculated from the Cr-Cu-Zr phase diagram (ref. 18) using the lever rule and compared to the image analysis results in table 2. There are differences in the two sets of values that can be as much as a 24.7 percent difference for the volume fraction of Cr. The error in the image analysis results is likely 5 percent or less, so there is an indication that a further refinement of the calculated Cr-Cu-Zr phase diagram may be required.

While the addition of a fourth element may dramatically change the interactions between Cu, Cr, and Nb, one implication of this work is that adding Zr to the Cu-Cr-Nb system may form a Cu-Zr matrix and Cr_2Nb precipitates. If the amount of Zr is limited to approximately 0.1 at.% Zr and the Zr does not dissolve into the Cr_2Nb or react with it, the composition of the matrix will approximate the commercial alloy AMZIRC. This addition may serve to improve the LCF and creep properties of Cu-Cr-Nb alloys such as GRCop-84 with only a small decrease in thermal conductivity (ref. 28) based upon the differences observed between pure Cu and AMZIRC.

Conversely, the addition of a small amount of Nb to the Cu-Cr-Zr alloy may change the activities and free energies of formation sufficiently so that Cr_2Zr will form. The work by Glazov et al. (refs. 15 and 16) and Zakharov et al. (ref. 17) where Cr_2Zr was found and a Cu-Cr_2Zr pseudobinary phase diagram was postulated may have been influenced by impurities. Nb will react strongly with Cr to form Cr_2Nb in the liquid phase for Cu-Cr-Nb alloys (refs. 1 and 29). These precipitates may act as favorable nucleation sites for Cr_2Zr given the similarities in crystallography and lattice spacings.

Summary and Conclusion

A cast Cu-6.15 wt% Cr-5.25 wt% Zr (Cu-7.5 at.% Cr-3.7 at.% Zr) alloy was examined in the as-cast condition and after an extended heat treatment at 875 °C. In both cases three phases were identified—Cu, Cr, and Cu_5Zr. In neither case was the desired Cr_2Zr phase observed. These results are consistent with the most recent experimental and computational work by Zeng et al. (refs. 18 and 19) on the Cr-Cu-Zr phase diagram.

While Zr and Nb are chemically similar in many respects and form crystallographically analogous intermetallic compounds with Cr with the same atomic ratio, it was concluded that there are sufficient differences that prevent the formation of the desired phases and microstructure in Cu-Cr-Zr alloys. This appears to make them unsuitable candidates for additional development as a potential supplement or replacement to GRCop-84 in rocket engine applications.

References

1. Ellis, D.L.; and Michal, G.M.: Precipitation Strengthened High Strength, High Conductivity Cu-Cr-Nb Alloys Produced by Chill Block Melt Spinning. NASA CR–185144, 1989.
2. Ellis, David L.; and Michal, Gary M.: Mechanical and Thermal Properties of Two Cu-Cr-Nb Alloys and NARloy-Z; Final Report. NASA CR–198529, 1996.
3. Ellis, David L.; Keller, Dennis J.; and Nathal, Michael: Thermophysical Properties of GRCop-84; Final Report. NASA/CR—2000-210055, 2000.
4. Chakrabarti, D.J.; and Laughlin, D.E.: The Cr-Cu (Chromium-Copper) System. Bull. Alloy Phase Diagrams, vol. 5, no. 1, 1984, pp. 59–68.
5. Chakrabarti, D.J.; and Laughlin, D.E.: The Cu-Nb (Copper-Niobium) System. Bull. Alloy Phase Diagrams, vol. 2, no. 4, 1982, pp. 455–460.
6. Goldschmidt, H.J.; and Brand, J.A.: The Constitution of the Chromium Niobium Molybdenum System. J. Less Common. Met., vol. 3, no. 1, 1961, pp. 44–61.
7. Ellis, David L.: Aerospace Structural Materials Handbook Supplement GRCop-84. 2004. Available from the NASA Center for AeroSpace Information.
8. Taubenblat, P.W.; Smith, W.E.; and Graviano**,** A.R.: Properties and Applications of High Strength, High Conductivity Coppers and Copper Alloys. High Conductivity Copper and Aluminum Alloys, Evan Ling and Pierre W. Taubenblat, eds., The Metallurgical Society of the AIME, Warrendale, PA, 1984, pp. 19–29.
9. A Survey of Properties and Applications of OFHC Brand Copper. AMAX Copper, Inc., New York, NY, 1974.
10. Esposito, J.J.; and Zabora, R.: Thrust Chamber Life Prediction: Volume 1: Mechanical and Physical Properties of High Performance Rocket Nozzle Materials; Final Report. NASA CR–134806, 1975.
11. Brandes, E.A., ed.: Smithells Metals Reference Book. Sixth ed., Butterworths, London, 1983.
12. Powder Diffraction File. Set 6, Card 6–0612, Cr_2Zr, International Centre for Diffraction Data, Newtown, PA, 1967.
13. Powder Diffraction File. Set 47, Card 47–1639, Cr_2Nb, International Centre for Diffraction Data, Newtown, PA, 1967.

14. Arias, D.; and Abriata, J.P.: Cu-Zr Phase Diagram. Phase Diagrams of Binary Copper Alloys, P.R. Subramanian, D.J. Chakrabarti, and D.E. Laughlin, eds., ASM International, Materials Park, OH, 1994, pp. 497–502.
15. Glazov, V.M.; Zakharov, M.V.; and Stepanova, M.V.: Izk. Akad. Nauk SSSR, Otdel. Tekh., Nauk, vol. 1, 1956, p. 162.
16. Glazov, V.M.; Zakharov, M.V.; and Stepanova, M.V.: Izk. Akad. Nauk SSSR, Otdel. Tekh., Nauk, vol. 9, 1957, p. 123.
17. Zakharov, M.V.; Stepanova, M.V.; and Glazov, V.M.: Metall. Term. Obra. Metallov., vol. 3, 1957, p. 23.
18. Zeng, K.J.; and Hämäläinen, M.: A Theoretical-Study of the Phase-Equilibria in the Cu-Cr-Zr System. J. Alloys Compounds, vol. 220, issues 1–2, 1995, pp. 53–61.
19. Zeng, K.J.; Hämäläinen M.; and Lilius, K.: Phase-Relationships in Cu-Rich Corner of the Cu-Cr-Zr Phase-Diagram. Scripta Metal. Mater., vol. 32, no. 12, 1995, pp. 2009–2014.
20. Allred, A.L.: Electronegativity Values From Thermochemical Data. J. Inorg. Nucl. Chem., vol. 17, nos. 3–4, 1961, pp. 215–221.
21. Donachie, M.J. Jr.: Investigation of Copper-Rich Portion of Copper-Zirconium Phase Diagram by Electron-Probe Microanalysis. J. Inst. Met., vol. 92, no. 6, 1964, p. 180.
22. Glimois, J.L.; Forey, P.; and Feron, J.L.: Structural and Physical Studies of Copper-Rich Alloys in the Cu-Zr System. J. Less Common Met., vol. 113, no. 2, 1985, pp. 213–224.
23. Forey, P.; Glimois, J.L.; and Feron, J.L.: Structural Study of Ternary $(Ni_{1-x}Cu_x)5Zr$ Alloys. J. Less Common Met., vol. 124, 1986, pp. 21–27.
24. Phillips, V.A.: Electron Microscope Observations on Precipitation in a Cu-1.07% Zr Alloy. Metallography, vol. 7, issue 2, 1974, pp. 137–155.
25. Forey, P., et al.: Synthesis, Characterization and Crystal-Structure of Cu5Zr. CR Hebd. Seances Acad. Sci. Ser. C, vol. 291, no. 6, 1980, pp. 177–178.
26. Lou, M. Y-W.; and Grant, N.J.: Identification of Cu5Zr Phase in Cu-Zr Alloys. Metall. Trans. A, vol. 15, no. 7, 1984, pp. 1491–1493.
27. Powder Diffraction File. Set 40, Card 40–1322, Cu_5Zr, International Centre for Diffraction Data, Newtown, PA, 1990, p. 496.
28. Horn, D.D.; and Lewis, H.F.: Property Investigation of Copper Base Alloys at Ambient and Elevated Temperatures. AEDC–TR–65–72, 1965.
29. Ellis, D.L.; and Michal, G.M.: Formation of Cr and Cr2Nb Precipitates in Rapidly Solidified Cu-Cr-Nb Ribbon. ULTRD, vol. 30, nos. 1–2, 1989, pp. 210–216.

REPORT DOCUMENTATION PAGE

Form Approved
OMB No. 0704-0188

1. AGENCY USE ONLY (*Leave blank*)	2. REPORT DATE	3. REPORT TYPE AND DATES COVERED
	February 2006	Technical Memorandum

4. TITLE AND SUBTITLE

Observations of a Cast Cu-Cr-Zr Alloy

5. FUNDING NUMBERS

WBS–22–617–44–20

6. AUTHOR(S)

David L. Ellis

7. PERFORMING ORGANIZATION NAME(S) AND ADDRESS(ES)

National Aeronautics and Space Administration
John H. Glenn Research Center at Lewis Field
Cleveland, Ohio 44135–3191

8. PERFORMING ORGANIZATION REPORT NUMBER

E–15286

9. SPONSORING/MONITORING AGENCY NAME(S) AND ADDRESS(ES)

National Aeronautics and Space Administration
Washington, DC 20546–0001

10. SPONSORING/MONITORING AGENCY REPORT NUMBER

NASA TM—2006-213968

11. SUPPLEMENTARY NOTES

Responsible person, David L. Ellis, organization code RMM, 216–433–8736.

12a. DISTRIBUTION/AVAILABILITY STATEMENT

Unclassified - Unlimited
Subject Category: 26

Available electronically at http://gltrs.grc.nasa.gov

This publication is available from the NASA Center for AeroSpace Information, 301–621–0390.

12b. DISTRIBUTION CODE

13. ABSTRACT ***(Maximum 200 words)***

Prior work has demonstrated that Cu-Cr-Nb alloys have considerable advantages over the copper alloys currently used in regeneratively cooled rocket engine liners. Observations indicated that Zr and Nb have similar chemical properties and form very similar compounds. Glazov and Zakharov et al. reported the presence of Cr_2Zr in Cu-Cr-Zr alloys with up to 3.5 wt% Cr and Zr though Zeng et al. calculated that Cr_2Zr could not exist in a ternary Cu-Cr-Zr alloy. A cast Cu-6.15 wt% Cr-5.25 wt% Zr alloy was examined to determine if the microstructure developed would be similar to GRCop-84 (Cu-6.65 wt% Cr-5.85 wt% Nb). It was observed that the Cu-Cr-Zr system did not form any Cr_2Zr even after a thermal exposure at 875 °C for 176.5 h. Instead the alloy consisted of three phases: Cu, Cu_5Zr, and Cr.

14. SUBJECT TERMS

Cooper; Microstructure; Intermetallics; Cast alloy; Phase diagrams

15. NUMBER OF PAGES

15

16. PRICE CODE

17. SECURITY CLASSIFICATION OF REPORT	18. SECURITY CLASSIFICATION OF THIS PAGE	19. SECURITY CLASSIFICATION OF ABSTRACT	20. LIMITATION OF ABSTRACT
Unclassified	Unclassified	Unclassified	